Calculation of spin-polarized positronium-helium ($2\,^3S$) and electron-helium ($2\,^3S$) scattering

Yi Zhang,[1,2] Meng-Shan Wu,[1,*] Ying Qian,[3] Kalman Varga,[4] and Jun-Yi Zhang[1]

[1]*State Key Laboratory of Magnetic Resonance and Atomic and Molecular Physics, Innovation Academy for Precision Measurement Science and Technology, Chinese Academy of Sciences, Wuhan 430071, China*

[2]*University of Chinese Academy of Sciences, Beijing 100049, China*

[3]*Department of Computer Science and Technology, East China Normal University, Shanghai 200062, China*

[4]*Department of Physics and Astronomy, Vanderbilt University, Nashville, Tennessee 37235, USA*

(Received 24 February 2021; accepted 16 April 2021; published 5 May 2021)

Low-energy properties of spin-polarized electron-helium ($2\,^3S$) and spin-polarized positronium-helium ($2\,^3S$) scattering are calculated using the modified confined variational method. To take the van der Waals interaction into consideration, the van der Waals coefficient between positronium and helium ($2\,^3S$) is calculated using the explicitly correlated Gaussian basis. Compared with the ground state noble gases, the larger scattering length and zero pickoff annihilation rate indicates that He($2\,^3S$) may be a more suitable cooling gas. In the energy range we considered, no similarity is found for the S-wave cross sections between these two scatterings. A Ramsauer-Townsend minimum is observed in spin-polarized electron-helium($2\,^3S$) scattering due to the large polarization of metastable helium. This may open a new way to find and study the Ramsauer-Townsend effect.

DOI: 10.1103/PhysRevA.103.052803

I. INTRODUCTION

The positronium (Ps) "atom" is a hydrogenlike bound system of an electron and a positron. This special leptonic atom is suitable for testing the theory of quantum electrodynamics and exploring physics beyond the standard model [1–7]. Since the projectile has a composite structure, Ps scattering is supposed to be different from bare electron scattering. However, similarities of the total cross sections between Ps and electron scattering by He, Ar, Kr, Xe, H_2, N_2, O_2, and SF_6 have been observed [8,9], which suggests that the contribution of the electron is dominant in Ps scattering at intermediate energies. Moreover, extremely small cross sections were observed in the scattering of slow Ps by Ar and Xe, which approach those of the Ramsauer-Townsend minima for electron projectiles [10,11].

Helium (He) is the lightest rare gas atom, and the scattering properties of electron-He (e-He) [12–19] and Ps-He [20–27] have been extensively studied both theoretically and experimentally. However, few works have focused on e or Ps scattering by excited He($2\,^3S$) [28–34]. In this work, we carried out calculations on the low-energy properties of spin-polarized electron-He* (sp-e-He*) and spin-polarized Ps-He* (sp-Ps-He*) scattering, where He* denotes He($2\,^3S$). Here, sp-Ps-He* means that the spins of the positron and three electrons have the same orientation, and similarly for sp-e-He* [35,36]. Due to the same spin alignment, the pickoff annihilation rate of sp-Ps-He* scattering is zero. The pickoff annihilation rate represents the probability that the positron in Ps annihilates with an electron in the atom (the positron-electron pair should be in a spin singlet state) during the scattering process [24,25]. This rate is essential for understanding the complex processes involved in the thermalization of Ps in gases. It is noted that the fully spin-polarized ensemble of Ps [35], spin-polarized He* [37], high-density Ps gas [38], and tunable Ps beam [39–41] have already been achieved experimentally. Thus, the zero pickoff annihilation rate could enable the utilization of sp-Ps-He* scattering in future experiments. However, to the best of our knowledge, no theoretical study has been reported for this system. Additionally, the Ramsauer-Townsend effect could occur in sp-e-He* and sp-Ps-He* scattering due to the large polarization of He*, though it has not been found in e-He and Ps-He scattering [10,11,27]. In addition, the similarities of the total cross sections between sp-e-He* scattering and sp-Ps-He* scattering is an interesting topic and deserves additional research [8,42].

The confined variational method (CVM) proposed by Mitroy *et al.* [14] and further developed by Zhang *et al.* [43] is an *ab initio* method for studying low-energy elastic scattering problems. It has been successfully applied to investigate many few-body elastic scattering problems, including e-H, e^+-H, e-He, e^+-He, Ps-H, and Ps-H_2 [14,43–45]. Contrary to the original CVM, we recently developed a strategy that can effectively eliminate unphysical confinement effects and greatly reduce the computational cost [46]. A smaller confining radius R_0 is used, which can extend the CVM to non-S partial waves and higher energy scattering.

The purpose of the present work is to apply the modified CVM to calculate the low-energy phase shifts, scattering lengths, and cross sections for sp-e-He* and sp-Ps-He* scattering. Then, the Ramsauer-Townsend effect and similarities of the S-wave cross sections between these two systems are investigated. This paper is organized as follows. In Sec. II, the modified CVM is introduced. Our results are presented in Sec. III, where the van der Waals coefficient for sp-Ps-He*

*mswu@apm.ac.cn

is given in Sec. III A, the S-wave phase shifts are given in Sec. III B, the S-wave scattering lengths are given in Sec. III C, and the S-wave cross sections are given in Sec. III D. Finally, Sec. IV provides a conclusion. Phase shifts are expressed in radians, and atomic units (a.u.) are used throughout unless otherwise stated.

II. THEORY

Here we give a brief introduction to the modified CVM. More details could be found in Refs. [14,43,44,46]. Take the calculations of the phase shifts of sp-Ps-He* scattering as an example. In this work, we only consider the infinite nuclear mass case, i.e., the mass of the He nucleus is infinite. Thus, the reduced mass is 2. The potential between Ps and He* is supposed to be $V_1(\rho)$, where ρ is the distance between the He nucleus and the center of mass of Ps. For this many-body scattering problem, we do not know the explicit form of $V_1(\rho)$. The key idea of the CVM is to find a proper model potential V_2 that has the same phase shift as V_1. Thus the phase shift of the sp-Ps-He* scattering can be obtained from the scattering equation of V_2 instead of V_1. The one-dimension representation of the CVM calculation can by described by the following four Schrödinger equations:

$$\left(-\frac{1}{4}\frac{d^2}{d\rho^2}+\frac{L^2+L}{4\rho^2}+V_1(\rho)+v_{\rm cp}(\rho)\right)\phi_1=E^s\phi_1, \quad (1)$$

$$\left(-\frac{1}{4}\frac{d^2}{d\rho^2}+\frac{L^2+L}{4\rho^2}+V_2(\rho)+v_{\rm cp}(\rho)\right)\phi_2=E^s\phi_2, \quad (2)$$

$$\left(-\frac{1}{4}\frac{d^2}{d\rho^2}+\frac{L^2+L}{4\rho^2}+V_1(\rho)\right)\phi_1'=E^s\phi_1', \quad (3)$$

$$\left(-\frac{1}{4}\frac{d^2}{d\rho^2}+\frac{L^2+L}{4\rho^2}+V_2(\rho)\right)\phi_2'=E^s\phi_2', \quad (4)$$

where $E^s=k^2/4$ is the scattering energy and k is the momentum of the Ps. ϕ_1 is the bound state wave function of the real potential V_1 (between Ps and He*) under the confining potential $v_{\rm cp}$. ϕ_2 is the bound state wave function of the model potential V_2 under the confining potential. ϕ_1' is the scattering wave function of V_1, and ϕ_2' is the one of V_2. The adjustable model potential V_2 has the form

$$V_2(\rho)=\lambda e^{-\alpha\rho}-\frac{C_6}{\rho^6}(1-e^{-(\rho/\beta)^6}), \quad (5)$$

where λ, α, and β are adjustable parameters. Usually, α and β are fixed (in present work, $\alpha=0.5$ and $\beta=5.0$); thus, only λ is adjustable. $-C_6/(\rho^6)$ is the long-range van der Waals potential between Ps and He*, and C_6 is the van der Waals coefficient between them, which has not been reported. The confining potential $v_{\rm cp}$ has the form

$$\begin{aligned} v_{\rm cp}(\rho)&=0, \quad \rho<R_0,\\ v_{\rm cp}(\rho)&=G(\rho-R_0)^2, \quad \rho\geqslant R_0, \end{aligned} \quad (6)$$

where G is a tunable positive number. R_0 is chosen to ensure that the complicated short-range interaction between Ps and He* can be ignored outside the sphere of radius R_0. To achieve continuity of the four wave functions ϕ_1, ϕ_2, ϕ_1' and ϕ_2', their logarithmic derivatives

$$\Gamma_X(R_0)\equiv\frac{1}{X(R_0)}\frac{dX}{d\rho}\bigg|_{R_0} \quad (7)$$

must be the same at energy E^s and radius R_0 [14], i.e.,

$$\Gamma_{\phi_1}(R_0)=\Gamma_{\phi_2}(R_0)=\Gamma_{\phi_1'}(R_0)=\Gamma_{\phi_2'}(R_0). \quad (8)$$

This implies that the phase shift, as a function of $\Gamma_X(R_0)$, is exactly the same for Eqs. (3) and (4) at E^s.

To obtain the $k-$ and $L-$ dependent $v_{\rm cp}$ and V_2 (or G and λ), we carry out the following many-body calculations using the explicitly correlated Gaussian (ECG) basis [47]. First, the confining potential $V_{\rm cp}$ is added to the Hamiltonian of the sp-Ps-He* system so that it becomes a bound-state eigenvalue problem:

$$(H+V_{\rm cp})\Psi(\mathbf{r},\mathbf{s})=E\Psi(\mathbf{r},\mathbf{s}), \quad (9)$$

$$H=-\frac{1}{2}\sum_{i=1}^{4}\nabla_i^2+\sum_{i=1}^{4}\frac{Qq_i}{r_i}+\sum_{\substack{i,j=1\\ i<j}}^{4}\frac{q_iq_j}{|\mathbf{r}_j-\mathbf{r}_i|}, \quad (10)$$

where $\mathbf{r}_1$, $\mathbf{r}_2$, $\mathbf{r}_3$, and $\mathbf{r}_4$ are the position vectors of the three electrons and the positron relative to the fixed nucleus, $\mathbf{r}$ denotes $(\mathbf{r}_1,\mathbf{r}_2,\mathbf{r}_3,\mathbf{r}_4)$ collectively, and $\mathbf{s}$ denotes $(\mathbf{s}_1,\mathbf{s}_2,\mathbf{s}_3,\mathbf{s}_4)$, the spins of the three electrons and the positron. Additionally, q_i is the charge of the i-th lepton, and Q is the charge of the He nucleus. $\Psi(\mathbf{r},\mathbf{s})$ is the eigenfunction of $H+V_{\rm cp}$ corresponding to E, where E is the total energy of the original scattering system, including the ground state energy of He*, the ground state energy of Ps, and the kinetic energy of Ps. This means that $E=-2.175229378-0.25+E^s$. The eigenfunction $\Psi(\mathbf{r},\mathbf{s})$ can be expanded in terms of the ECG basis:

$$\varphi_n(\mathbf{r},\mathbf{s})=|\mathbf{v}|^{2K+L}\exp\left(-\tfrac{1}{2}\mathbf{r}^{\rm T}A_n\mathbf{r}\right)Y_{LM}(\mathbf{v})\chi(\mathbf{s}), \quad (11)$$

where $\mathbf{v}=u^{\rm T}\mathbf{r}$, with $u^{\rm T}=(u_1,u_2,u_3)$ being a global vector, $\chi(\mathbf{s})$ is the spin function, K is set to be less than or equal to the number of nodes of the wave function, A_n is a parameter matrix, L and M are the total orbital angular momentum and its z component, respectively, and Y_{LM} is the spherical harmonics.

The confining potential used in the original CVM is

$$V_{\rm cp}=\sum_{i=1}^{3}v_{\rm cp}(\rho_i), \quad (12)$$

where $\rho_i=|\mathbf{r}_i+\mathbf{r}_4|/2$ is the distance between the He nucleus and the center of mass of Ps. To eliminate unphysical confinement effects, we define the following judgment index between two basis functions φ_n and φ_m [46]:

$$s_i^{nm}=\frac{\langle\varphi_n|\Theta(r_{i4}-R_1)(r_{i4}-R_1)^2|\varphi_m\rangle}{\langle\varphi_n|\Theta(\rho_i-R_0)(\rho_i-R_0)^2|\varphi_m\rangle}, \quad (13)$$

where $r_{i4}=|\mathbf{r}_i-\mathbf{r}_4|$ is the distance between the i-th electron and positron in a confined Ps, R_1 is an adjustable number greater than $2a_0$, with a_0 being the Bohr radius, and Θ is the Heaviside step function. If the confining potential acts on the pseudo-Ps formed by the positron and the electron of He*, then r_{i4} will be much larger than the characteristic size $2a_0$ of Ps. This means that s_i^{nm} will be a large number when R_1 is set to $2a_0$ or slightly larger. We discard $\langle\varphi_n|V_{\rm cp}(\rho_i)|\varphi_m\rangle$ when s_i^{nm}

exceeds a specific threshold. In this work, R_1 is set equal to R_0, and thus, the specific threshold for s_i^{nm} is set to 1.0.

The CVM calculation contains the following three main steps. Firstly, the confining potential $V_{\rm cp}$ is added to the Hamiltonian of the original scattering problem [see Eq. (9)]. Parameter G is tuned to ensure a specific momentum k. For example, if we want to calculate the phase shift at $k = 0.1$, the scattering energy is $0.1^2/(2 \cdot 2) = 0.0025$, which means the total energy E should be tuned to be $-2.175229378 - 0.25 + 0.1^2/(2 \cdot 2) = -2.422729378$. Then G is obtained. Secondly, we solve Eq. (2) to find the appropriate model potential V_2 [Eq. (5)]. In this step, there is an adjustable parameter: λ (α and β are fixed). In this paper, for simplicity, α and β are fixed. For α, we checked the range [0.4, 1.0], which gives the same phase shift. For β, we checked the range [4, 10], which also gives the same phase shift. Since G has been obtained in the first step, only λ is tuned to ensure the same momentum k as in step one. Then λ is obtained, which means the appropriate model potential V_2 is found. At last, we calculate the exact phase shift of Ps-He* scattering δ_L^k from the model potential V_2 instead of V_1. This is done by solving the scattering equation of V_2 (Eq. (4)), i.e., by applying an integration procedure and a least-squares fit between $\phi_2'(\rho)$ and $A\sin(k\rho - L\pi/2 + \delta_L^k)$ for $\rho \to \infty$.

III. RESULTS

A. Van der Waals coefficient between Ps and He*

When the distance between Ps and He* is large enough, the complicated short-range interaction will be negligibly small; then, the long-range van der Waals interaction will be dominant. The van der Waals interaction represents the interaction between two electrically neutral but polarizable systems, which can be denoted as $V(\rho) \approx -C_6/\rho^6$. The van der Waals coefficient C_6 between Ps and He* is needed in model potential V_2 [see Eq. (5)], but it has not been reported. Thus, we perform a calculation to estimate C_6 using the oscillator strength sum rule [49]:

$$C_6 = \frac{3}{2}\sum_{ij}\frac{f_{0i}^A f_{0j}^B}{\epsilon_{0i}^A \epsilon_{0j}^B\left(\epsilon_{0i}^A + \epsilon_{0j}^B\right)}, \tag{14}$$

where ϵ_{0i}^A is the transition energy between the i-th excited state and the ground state of atom A, and atoms A and B represent Ps and He*, respectively. f_{0i}^A is the corresponding 2^1-pole oscillator strength and is defined by

$$f_{0i}^A = \frac{8\pi}{3}\epsilon_{0i}^A \left|\langle\psi_0^A\left|\sum_n \hat{r}_n P_1(\cos\theta_n)\right|\psi_i^A\rangle\right|, \tag{15}$$

where ψ_0^A and ψ_i^A are the wave functions of the ground state and the i-th excited state of atom A, respectively. $P_1(\cos\theta_n)$ is the Legendre polynomial.

In this work, the energy ϵ_i^A and wave function ψ_i^A are calculated using the ECG basis combined with the stochastic variational method (SVM) [47]. Then, the calculations of oscillator strength f_{0i}^A can be easily generalized for an N-body system since the matrix elements in Eq. (15) are calculated analytically using the ECG basis. Note that the summation in Eq. (14) should include all bound and continuum states. To examine the accuracy of our calculated energies, wave functions and oscillator strengths, we calculate the polarization of Ps and He* in advance. The polarization can also be calculated using the oscillator strength sum rule:

$$\alpha^A = \sum_i \frac{f_{0i}^A}{\left(\epsilon_{0i}^A\right)^2}. \tag{16}$$

The maximum numbers of basis functions used for the expansion of Ps and He* are 50 and 2500, respectively. The calculated polarization of Ps is 36.0000000001, which agrees well with the exact value 36. The calculated polarization of He* is 315.631470, which agrees well with the calculated value of Yan *et al.* of 315.631468 [50]. These results show that the energies, wave functions, and oscillator strengths we calculated are of high quality and are suitable for C_6 calculation.

TABLE I. Convergence test of the van der Waals coefficient C_6 (in a.u.) for Ps-He and sp-Ps-He* scattering as the size of the He or He* basis set N increases.

N	C_6(Ps-He)	C_6(Ps-He*)
1500	13.3657399	632.742736
1600	13.3657403	632.742409
1800	13.3657408	632.743022
2000	13.3657409	632.743219
2200	13.3657410	632.743236
2500	13.3657411	632.743238
	13.365741777 [48]	

Table I shows the convergence tests for C_6 of Ps-He and sp-Ps-He* as the size of the basis set N increases. N refers to the basis size of He and He* for Ps-He and sp-Ps-He*, respectively. The basis size used for Ps is 50. C_6 converges smoothly as N increases, and both values have eight significant digits. The van der Waals coefficient of Ps-He calculated by Kar and Ho using the Hylleraas basis is 13.365741777, which is in good agreement with our value. Thus, the C_6 we calculated for sp-Ps-He* is precise enough to be used in the following scattering calculations.

B. Phase shifts for sp-*e*-He* and sp-Ps-He* scattering

The CVM has been used to study various few-body elastic scatterings, including e-H, e^+-H, e-He, e^+-He, Ps-H, Ps-He, and Ps-H_2 [14,24,43–45], which all have a small polarization or van der Waals coefficient. In our calculations, R_0 should be large enough to ensure that the van der Waals potential $-C_6/\rho^6$ or the polarization potential $-\alpha/(2\rho^4)$ is dominant. However, a larger R_0 will entail higher computational costs. Since the polarization of He* is large, the confining potential range R_0 and the size of the ECG basis N should be chosen carefully. Thus, convergence tests of the phase shifts with respect to R_0 and N are performed in advance, and the results are shown in Tables II and III, respectively. According to Table II, the phase shifts converge smoothly as R_0 increases. $R_0 = 25$ gives three convergent digits for the $\delta_0^{0.05}$ of sp-e-He* scattering and $\delta_0^{0.1}$ of sp-Ps-He* scattering. Thus, $R_0 = 25$ is used for the calculations of sp-e-He* scattering and sp-Ps-He*

TABLE II. Convergence test of the scattering phase shifts (δ_L^k, in radians) for sp-e-He* and sp-Ps-He* scattering as the confining radius R_0 increases.

R_0	$\delta_0^{0.05}$(sp-e-He*)	$\delta_0^{0.1}$(sp-Ps-He*)
23	0.19164	−0.35430
24	0.19137	−0.35444
25	0.19123	−0.35452

scattering. According to Table III, $N = 2400$ gives three convergent digits for the $\delta_0^{0.05}$ of sp-e-He* scattering and $\delta_0^{0.1}$ of sp-Ps-He* scattering; thus, $N = 2400$ is used for all our calculations.

The calculated phase shifts for $k = 0.04 - 0.12$ of sp-e-He* scattering and a comparison with the e-He scattering phase shifts [13] are shown in Table IV. The calculated phase shifts for $k = 0.06 - 0.12$ of sp-Ps-He* scattering and a comparison with the Ps-He scattering phase shifts [25] are shown in Table V. According to Table IV, the phase shift of sp-e-He* scattering changes sign from positive at $k = 0.08$ to negative at $k = 0.09$, while the phase shifts of e-He scattering are all negative. The positive phase shifts mean that for $k \leqslant 0.08$, the interaction between electron and He* is attractive, which is due to the large polarization of He*. For $k \geqslant 0.1$, the phase shift of sp-e-He* scattering decreases more quickly than that of e-He scattering. According to Table V, the phase shifts of sp-Ps-He* scattering are smaller than those of Ps-He scattering. Comparing the phase shifts in Table IV with those in Table V, we can infer that electron scattering is not dominant in Ps for sp-Ps-He* and Ps-He scattering at $k < 0.12$.

C. Scattering lengths for sp-e-He* and sp-Ps-He* scattering

The S-wave scattering length A_0 can be obtained by fitting the calculated phase shift δ_L^k at low k to the effective range expansion

$$k \cot \delta_0^k = -\frac{1}{A_0} + \frac{R_e k^2}{2}, \tag{17}$$

where R_e is the corresponding effective range. When the long-range polarization potential is taken into consideration, the modified effective range expansion [51] for sp-e-He* scattering is

$$\tan \delta_0^k = -A_0 k\left[1 + \frac{4\alpha k^2}{3}\ln(k)\right] - \frac{\pi\alpha k^2}{3} + Dk^3 + Fk^4, \tag{18}$$

TABLE III. Convergence test of the scattering phase shifts (δ_L^k, in radians) for sp-e-He* and sp-Ps-He* scattering as the size of the basis set N increases.

N	$\delta_0^{0.05}$(sp-e-He*)	$\delta_0^{0.1}$(sp-Ps-He*)
2000	0.19148	−0.35424
2200	0.19134	−0.35442
2400	0.19123	−0.35452

TABLE IV. Phase shifts (δ_L^k, in radians) of sp-e-He* scattering calculated with the present CVM, and comparison with those of e-He scattering. a^b abbreviates $a \times 10^b$.

k(a.u.)	δ_0^k(sp-e-He*)	δ_0^k(e-He) [13]
0.04	2.355^{-1}	-4.926^{-2}
0.05	1.912^{-1}	-6.207^{-2}
0.06	1.360^{-1}	-7.503^{-2}
0.07	7.460^{-2}	-8.815^{-2}
0.08	9.784^{-3}	-1.014^{-1}
0.09	-5.694^{-2}	-1.147^{-1}
0.1	-1.246^{-1}	-1.282^{-1}
0.12	-2.619^{-1}	-1.554^{-1}

where $\alpha = 315.631470$ is the polarization of He*, and D and F are additional fitting parameters. Similarly, when the long-range van der Waals potential is taken into consideration, the modified effective range expansion [51] for sp-Ps-He* scattering is

$$k \cot \delta_0^k = -\frac{1}{A_0} + \frac{R_e k^2}{2} - \frac{4\pi C_6 k^3}{15(A_0)^2} - \frac{16 C_6}{15 A_0} k^4 \ln k, \tag{19}$$

where $C_6 = 632.743238$ is the calculated van der Waals coefficient in Table I.

The obtained scattering lengths of sp-e-He* and sp-Ps-He* scattering are shown in Table VI. For sp-e-He* scattering, the scattering lengths obtained with Eqs. (17) and (18) at $k = 0.04 - 0.07$ are 4.65 and −21.77, respectively. This shows that the addition of the long-range polarization potential effect has a very large effect on the scattering length due to the large polarization of He*. When the fitting range becomes $0.04 - 0.12$, the obtained scattering length is −26.95. Since the effective range expansions are more suitable for low k, our recommended value for the scattering length of sp-e-He* scattering is −21.77. The scattering length of e-He scattering is 1.1835 [13], whose absolute value is smaller than that of sp-e-He* scattering.

For sp-Ps-He* scattering, the scattering lengths obtained with Eqs. (17) and (19) at $k = 0.06 - 0.12$ are 3.47 and 3.56, respectively. Although sp-Ps-He* scattering has a large C_6, the effect of the van der Waals potential on the scattering length is smaller than the effect of the polarization potential on the scattering length of sp-e-He* scattering. This can be explained by $(\alpha)^{1/4} > (C_6)^{1/6}$. For example, at $R_0 = 25$, $\alpha/25^4 > C_6/25^6$, indicating that the polarization interaction is stronger. Our recommended value for the scattering length of sp-Ps-He* scattering is 3.56. The scattering lengths for Ps

TABLE V. Phase shifts (δ_L^k, in radians) of sp-Ps-He* scattering calculated with the present CVM, and comparison with those of Ps-He scattering. a^b abbreviates $a \times 10^b$.

k(a.u.)	δ_0^k(sp-Ps-He*)	δ_0^k(Ps-He) [25]
0.06	-2.101^{-1}	-1.019^{-1}
0.08	-2.812^{-1}	-1.357^{-1}
0.1	-3.545^{-1}	-1.693^{-1}
0.12	-4.286^{-1}	-2.028^{-1}

TABLE VI. Extracted S-wave scattering lengths (A_0, in a.u.) of sp-e-He* and sp-Ps-He* scattering.

	k(a.u.)	A_0
sp-e-He* Eq. (17)	0.04–0.07	4.65
sp-e-He* Eq. (18)	0.04–0.07	−21.77
sp-e-He* Eq. (18)	0.04–0.12	−26.95
sp-Ps-He* Eq. (17)	0.06–0.12	3.47
sp-Ps-He* Eq. (19)	0.06–0.12	3.56

scattering by He, Ne, Ar, Kr, and Xe are 1.566 [24], 1.65, 2.0, 2.3, and 2.6 [26], respectively, which are all smaller than that of sp-Ps-He* scattering. In addition, the pickoff annihilation rate of sp-Ps-He* scattering is zero. Thus, He($2\,^3S$) may be a more suitable cooling gas compared with the ground state noble gases.

D. *S*-wave cross-sections for sp-*e*-He* and sp-Ps-He* scattering

The S-wave cross sections of sp-e-He* and sp-Ps-He* scattering are presented in Fig. 1. The S-wave cross sections of sp-Ps-He* are approximately $48\pi a_0^2$ in the Ps momentum range of 0.06−0.12, where a_0 is the Bohr radius. No similarity is found between sp-e-He* and sp-Ps-He* scattering, regardless of whether the momentum or velocity is taken as the X axis [8]. The S-wave cross sections of sp-e-He* have a minimum around $k = 0.08$, which seems to be "target transparency" [10]. This phenomenon has been observed in electron scattering by heavy atoms Ar, Kr, and Xe and in positron scattering by He and Ne, which is now referred to as the Ramsauer-Townsend effect [9–11,27,52–54]. A Ramsauer-Townsend minimum of $0.016a_0^2$ was found in the electron scattering by beryllium at 0.0029 eV [54]. Extremely small cross sections were observed in the scattering of slow Ps by Ar and Xe, which approach those of the Ramsauer-Townsend minima for electron projectiles [10]. For e-He and Ps-He scattering, no Ramsauer-Townsend minima have been observed due to their positive scattering lengths and similarly for sp-Ps-He* scattering, which has a scattering length of 3.56. The total cross section can be calculated by summing over all partial-wave contributions as $\sum_L 4\pi(2L+1)\sin^2\delta_L/k^2$. Although we only calculated the S-wave phase shifts, the S-wave scattering is known to dominate in the low energy range. Since the S-wave phase shift goes through zero between $k = 0.08$ and 0.09, the Ramsauer-Townsend minimum occurs for sp-e-He* scattering. Our present work provides evidence that the Ramsauer-Townsend minimum can occur for the scattering of electrons by light atoms. Since He* in sp-e-He* scattering has a large polarization of $\alpha = 315.63147$, which is larger than the polarizations of Ne ($\alpha_{Ne} = 2.669$), Ar ($\alpha_{Ar} = 11.08$), Kr ($\alpha_{Kr} = 16.79$) and Xe ($\alpha_{Xe} = 27.16$) [55], the scattering of electron by excited atoms with large polarization could give rise to the Ramsauer-Townsend effect.

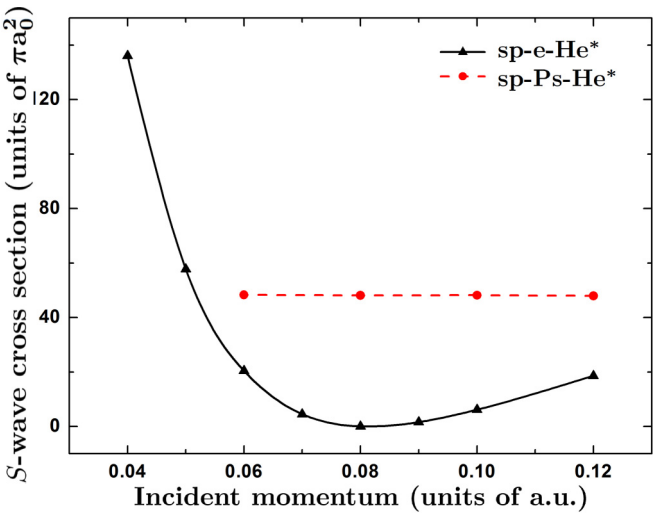

FIG. 1. S-wave cross sections of sp-e-He* and sp-Ps-He* scattering. The momentum refers to the momentum of an electron or Ps, respectively.

IV. CONCLUSION

The low-energy phase shifts, scattering lengths, and elastic cross sections of sp-e-He* and sp-Ps-He* scattering are calculated using the modified CVM combined with the ECG basis. The van der Waals coefficient between Ps and He* we calculated is 632.743238. The S-wave phase shift of sp-e-He* scattering goes through zero between $k = 0.08$ and 0.09. Using the modified effective range expansion, the extracted scattering lengths are −26.95 and 3.56 for sp-e-He* and sp-Ps-He*, respectively. Compared with the ground state noble gases, the larger scattering length and zero pickoff annihilation rate indicates that He($2\,^3S$) may be a more suitable cooling gas. No similarity of the S-wave cross sections between these two scatterings has been found at $k < 1.2$. A Ramsauer-Townsend minimum is observed between $k = 0.08$ and 0.09 in sp-e-He* scattering due to the large polarization of He*. Our present work provides evidence that the Ramsauer-Townsend effect can occur for the scattering of electrons by light atoms, which may open a new way to find and study this effect.

ACKNOWLEDGMENTS

We thank T.-Y. Shi and H.-L. Han for useful discussions and suggestions. This work was supported by the National Natural Science Foundation of China under Grants No. 11704399 and No. 11934014, by the Strategic Priority Research Program of the Chinese Academy of Sciences under Grant No. XDB21030300, and by the National Key Research and Development Program of China under Grant No. 2017YFA0304402.

[1] S. G. Karshenboim, Phys. Rep. **422**, 1 (2005).
[2] T. Yamazaki, A. Miyazaki, T. Suehara, T. Namba, S. Asai, T. Kobayashi, H. Saito, I. Ogawa, T. Idehara, and S. Sabchevski, Phys. Rev. Lett. **108**, 253401 (2012).
[3] G. S. Adkins, M. Kim, C. Parsons, and R. N. Fell, Phys. Rev. Lett. **115**, 233401 (2015).
[4] G. Gabrielse, R. Kalra, W. S. Kolthammer, R. McConnell, P. Richerme, D. Grzonka, W. Oelert, T. Sefzick, M. Zielinski,

D. W. Fitzakerley, M. C. George, E. A. Hessels, C. H. Storry, M. Weel, A. Müllers, and J. Walz (ATRAP Collaboration), Phys. Rev. Lett. **108**, 113002 (2012).
[5] A. S. Kadyrov, C. M. Rawlins, A. T. Stelbovics, I. Bray, and M. Charlton, Phys. Rev. Lett. **114**, 183201 (2015).
[6] C. Frugiuele, J. Pérez-Ríos, and C. Peset, Phys. Rev. D **100**, 015010 (2019).
[7] L. Gurung, T. J. Babij, S. D. Hogan, and D. B. Cassidy, Phys. Rev. Lett. **125**, 073002 (2020).
[8] S. J. Brawley, S. Armitage, J. Beale, D. E. Leslie, A. I. Williams, and G. Laricchia, Science **330**, 789 (2010).
[9] I. I. Fabrikant and G. F. Gribakin, Phys. Rev. Lett. **112**, 243201 (2014).
[10] S. J. Brawley, S. E. Fayer, M. Shipman, and G. Laricchia, Phys. Rev. Lett. **115**, 223201 (2015).
[11] S. E. Fayer, D. M. Newson, S. J. Brawley, A. Loreti, R. Kadokura, T. J. Babij, J. Lis, M. Shipman, and G. Laricchia, Phys. Rev. A **100**, 062709 (2019).
[12] B. Bederson and L. J. Kieffer, Rev. Mod. Phys. **43**, 601 (1971).
[13] R. K. Nesbet, Phys. Rev. A **20**, 58 (1979).
[14] J. Mitroy, J. Y. Zhang, and K. Varga, Phys. Rev. Lett. **101**, 123201 (2008).
[15] D. E. Golden and H. W. Bandel, Phys. Rev. **138**, A14 (1965).
[16] T. S. Stein, W. E. Kauppila, V. Pol, J. H. Smart, and G. Jesion, Phys. Rev. A **17**, 1600 (1978).
[17] R. E. Kennerly and R. A. Bonham, Phys. Rev. A **17**, 1844 (1978).
[18] L. S. Frost and A. V. Phelps, Phys. Rev. **136**, A1538 (1964).
[19] K. Shigemura, M. Kitajima, M. Kurokawa, K. Toyoshima, T. Odagiri, A. Suga, H. Kato, M. Hoshino, H. Tanaka, and K. Ito, Phys. Rev. A **89**, 022709 (2014).
[20] K. F. Canter, J. D. McNutt, and L. O. Roellig, Phys. Rev. A **12**, 375 (1975).
[21] Y. Nagashima, T. Hyodo, K. Fujiwara, and A. Ichimura, J. Phys. B **31**, 329 (1998).
[22] M. Skalsey, J. J. Engbrecht, C. M. Nakamura, R. S. Vallery, and D. W. Gidley, Phys. Rev. A **67**, 022504 (2003).
[23] J. J. Engbrecht, M. J. Erickson, C. P. Johnson, A. J. Kolan, A. E. Legard, S. P. Lund, M. J. Nyflot, and J. D. Paulsen, Phys. Rev. A **77**, 012711 (2008).
[24] J. Y. Zhang and J. Mitroy, Phys. Rev. A **78**, 012703 (2008).
[25] D. G. Green, A. R. Swann, and G. F. Gribakin, Phys. Rev. Lett. **120**, 183402 (2018).
[26] A. R. Swann and G. F. Gribakin, Phys. Rev. A **97**, 012706 (2018).
[27] R. S. Wilde and I. I. Fabrikant, Phys. Rev. A **98**, 042703 (2018).
[28] W. G. Wilson and W. L. Williams, J. Phys. B **9**, 423 (1976).
[29] L. J. Uhlmann, R. G. Dall, A. G. Truscott, M. D. Hoogerland, K. G. H. Baldwin, and S. J. Buckman, Phys. Rev. Lett. **94**, 173201 (2005).
[30] D. Husain, A. L. Choudhury, A. K. Rafiqullah, C. W. Nestor, and F. B. Malik, Phys. Rev. **161**, 68 (1967).
[31] R. C. Sklarew and J. Callaway, Phys. Rev. **175**, 103 (1968).
[32] I. Bray and D. V. Fursa, J. Phys. B **28**, L197 (1995).
[33] I. Khurana, R. Srivastava, and A. N. Tripathi, Phys. Rev. A **37**, 3720 (1988).
[34] W. Yuan-Cheng, Z. Ya-Jun, C. Yong-Jun, and M. Jia, Chin. Phys. Lett. **26**, 083401 (2009).
[35] D. B. Cassidy, V. E. Meligne, and A. P. Mills, Phys. Rev. Lett. **104**, 173401 (2010).
[36] D. B. Cassidy, Eur. Phys. J. D **72**, 53 (2018).
[37] L. Byron, R. Dall, W. Rugway, and A. Truscott, New J. Phys. **12**, 013004 (2010).
[38] D. B. Cassidy, S. H. M. Deng, R. G. Greaves, T. Maruo, N. Nishiyama, J. B. Snyder, H. K. M. Tanaka, and A. P. Mills, Phys. Rev. Lett. **95**, 195006 (2005).
[39] M. Shipman, S. Brawley, D. E. Leslie, S. Armitage, and G. Laricchia, Eur. Phys. J. D **66**, 96 (2012).
[40] M. Shipman, S. J. Brawley, L. Sarkadi, and G. Laricchia, Eur. Phys. J. D **68**, 75 (2014).
[41] M. Shipman, S. Armitage, J. Beale, S. J. Brawley, S. E. Fayer, A. J. Garner, D. E. Leslie, P. Van Reeth, and G. Laricchia, Phys. Rev. Lett. **115**, 033401 (2015).
[42] P. V. Reeth, D. Woods, S. J. Ward, and J. W. Humberston, J. Phys. B: At., Mol. Opt. Phys. **49**, 114001 (2016).
[43] J.-Y. Zhang, Z.-C. Yan, and U. Schwingenschlögl, Europhys. Lett. **99**, 43001 (2012).
[44] J. Y. Zhang, J. Mitroy, and K. Varga, Phys. Rev. A **78**, 042705 (2008).
[45] J.-Y. Zhang, M.-S. Wu, Y. Qian, X. Gao, Y.-J. Yang, K. Varga, Z.-C. Yan, and U. Schwingenschlögl, Phys. Rev. A **100**, 032701 (2019).
[46] M.-S. Wu, J.-Y. Zhang, X. Gao, Y. Qian, H.-H. Xie, K. Varga, Z.-C. Yan, and U. Schwingenschlögl, Phys. Rev. A **101**, 042705 (2020).
[47] J. Mitroy, S. Bubin, W. Horiuchi, Y. Suzuki, L. Adamowicz, W. Cencek, K. Szalewicz, J. Komasa, D. Blume, and K. Varga, Rev. Mod. Phys. **85**, 693 (2013).
[48] S. Kar and Y. Ho, Nucl. Instrum. Methods Phys. Res., Sect. B **266**, 526 (2008).
[49] A. Dalgarno and W. D. Davison, *Advances in Atomic and Molecular Physics*, edited by D. R. Bates and I. Estermann (Academic, New York, 1966), Vol. 2, p. 1.
[50] Z.-C. Yan, J. F. Babb, A. Dalgarno, and G. W. F. Drake, Phys. Rev. A **54**, 2824 (1996).
[51] M. R. Flannery, *Springer Handbook of Atomic, Molecular, and Optical Physics*, 2nd ed., edited by G. W. F. Drake (Springer, New York, 2006), p. 668.
[52] D. E. Golden and H. W. Bandel, Phys. Rev. **149**, 58 (1966).
[53] M. Adibzadeh and C. E. Theodosiou, At. Data Nucl. Data Tables **91**, 8 (2005).
[54] D. D. Reid and J. M. Wadehra, J. Phys. B **47**, 225211 (2014).
[55] T. M. Miller and B. Bederson, *Advances in Atomic and Molecular Physics*, edited by D. Bates and B. Bederson (Academic, New York, 1989), Vol. 25, p. 37.